

## **The Grandeur of Massive Star Formation — Revealed with ISAAC**

Hendrik Linz and Bringfried Stecklum

*TLS Tautenburg, Sternwarte 5, D-07778 Tautenburg, Germany*

Thomas Henning

*MPIA Heidelberg, Königstuhl 17, D-69117 Heidelberg, Germany*

Peter Hofner

*New Mexico Tech, 801 Leroy Place, Socorro, N.M. 87801, U.S.A.*

### **Abstract.**

We present selected results from our ongoing investigation of high-mass star-forming regions which are based on infrared observations with ESO's ISAAC camera at the 8.2-m ANTU VLT telescope. Although these young stellar objects comprise a high degree of complexity, our data enable us to disentangle these crowded regions. By means of broad- and narrow-band imaging between 1–5 micron we performed a thorough characterisation of the embedded population. Special emphasis was put on the importance of an accurate astrometry which has a major impact on the interpretation of the data. In the case of G9.62+0.19, we clarified the true nature of the infrared emission in the immediate vicinity of an hot molecular core (HMC). We unveil the counterpart of this HMC in the thermal infrared. For GGD27 IRS2, we found thermal emission at 3.8 and 4.7 micron caused by a deeply embedded object that is powering a large radio jet and has counterparts in our mid-infrared and VLA 7-mm data. The presented results mark a further step on the way to disclose the mechanisms of massive star formation. They demonstrate the value of sensitive infrared imaging with the current generation of IR cameras on 8-m-class telescopes.

## **1. Introduction**

The observations with the IR camera ISAAC (Moorwood 1997) were carried out in the first half of 2001 in service mode which was chosen to ensure that the ambient conditions meet our specifications, in particular the seeing demand. The narrow-band imaging in the 2.09  $\mu\text{m}$  filter was performed in polarimetric mode, i.e., with the Wollaston prism and the slit mask in the optical train. The dithering positions were chosen to achieve the full coverage of the field-of-view (FOV). Furthermore, these images served as continuum which had to be subtracted from the Br  $\gamma$  and H<sub>2</sub>(1–0)S1 narrow-band frames. For the data reduction we developed a general pipeline applicable to imaging data obtained

by ISAAC. The pipeline is written in the high-level IDL language, offering automated reduction together with the opportunity of flexibility. The aims of the measurements were as follows:

- Images in continuum filters ( $2.09 \mu\text{m}$ , L', nb\_M) to study the distribution of stars from the most massive to solar-type ones.
- Narrow-band imaging in Br  $\gamma$  ( $2.166 \mu\text{m}$ ) and Br  $\alpha$  ( $4.07 \mu\text{m}$ ) to deduce the amount and distribution of dust extinction.
- Images in the H<sub>2</sub>(1–0)S1 line ( $2.122 \mu\text{m}$ ) to search for shocks caused by winds and outflows from young stellar objects (YSOs).

Here, we show some results for two selected regions of high-mass star formation. Together with recent interferometric radio data, they demonstrate that high-resolution observations are required to overcome the confusion arising from the complexity of massive star formation.

## 2. Selected Results

### 2.1. G9.62+0.19 – A hot molecular core puzzles the IR observers

G9.62+0.19 is a complex of massive star formation regions ( $d \sim 5.7$  kpc). It comprises several YSOs in different evolutionary stages. An age gradient spans from western (older) to eastern (younger) regions (Hofner et al. 1996). The site harbours an hot molecular core (HMC), i.e., a very dense, warm and compact condensation of molecular gas (Cesaroni et al. 1994). NIR emission was found at the location of the HMC (Testi et al. 1998), in contradiction of HMC standard models (Osorio et al. 1999). The superior sensitivity and resolution of the new ISAAC data (VLT archive data for the filters J, H and Ks as well as our thermal infrared and NIR narrow-band data) lead to new conclusions:

**High resolution** (seeing  $0''.4 - 0''.6$ ): An intriguing substructure of the HMC region F has been revealed (decomposition into 3 IR objects, see Fig. 1).

**Highly accurate astrometry:** The peak positions of the HMC radio emission and of the strongest NIR peak in component F do not coincide (Fig. 1). A foreground NIR star (F2) at the HMC position fades at longer wavelengths. However, another source becomes apparent nearby (F4 in Fig. 1) which seems to be intrinsically associated with the HMC.

**Working hypothesis:** The finding of a pole-on molecular outflow probably driven by the HMC (Hofner et al. 2001) explains at least qualitatively why we can see at all thermal IR emission from the HMC – we benefit from the outflow's clearing effect.

**Still discussions:** Contrary to De Buizer et al. (2003), we find that also the compact 10-micron source found in the HMC region by several authors corresponds to the HMC. It is identical with object F4 (see Fig. 2).

Furthermore, there are localised regions of Br  $\gamma$  and H<sub>2</sub> emission as well as of reflected NIR continuum within G9.62+0.19 (Fig. 3) which demonstrates the complex structure of this region also on a larger scale.

The results of a comprehensive IR study about this star-forming region and its HMC will be given in Linz et al. (2003).

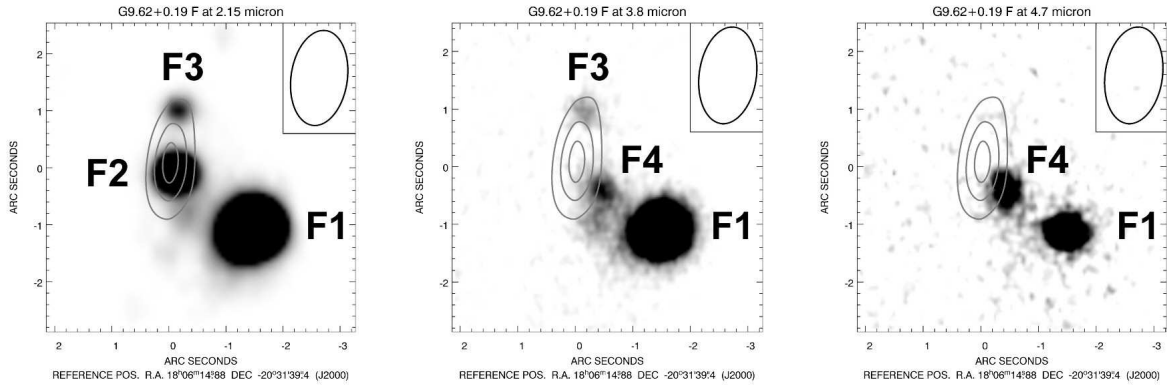


**Figure 1.** Immediate vicinity around the the Hot Core region F in G9.62+0.19. From left to right: Ks band, L' band, and narrow M band. The overlaid contours mark the peak position of the  $\text{NH}_3(5,5)$  emission of the hot molecular core (Hofner et al. 1994). The Ks band object F2 at this peak position turns out to be a foreground star that completely fades at longer wavelengths. But nearby we find strongly increasing emission (F4). We presume that this emission is associated with the Hot Core.

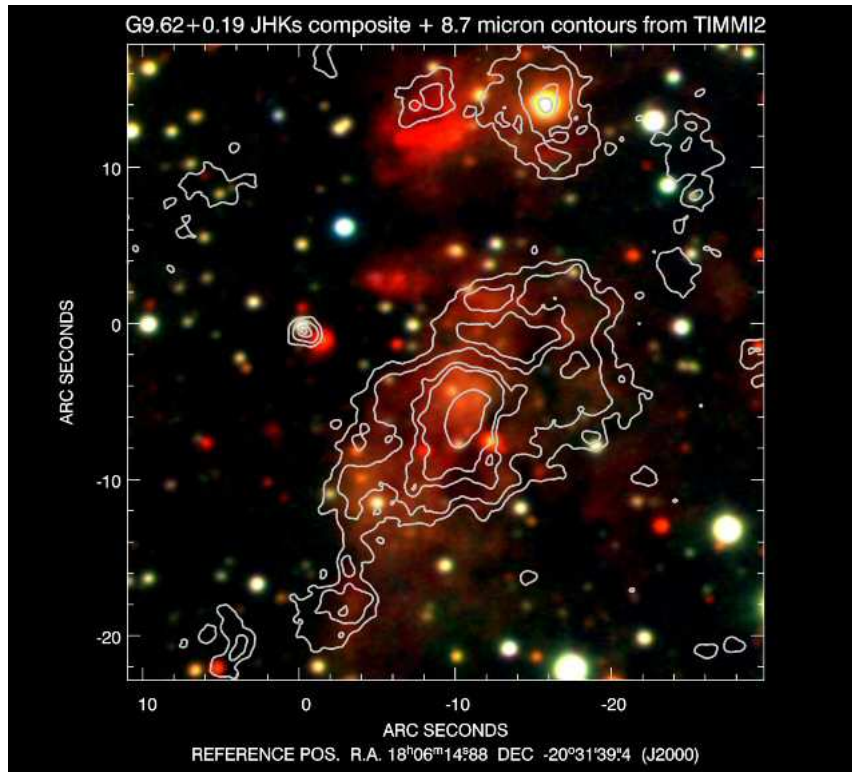


**Figure 2.** Colour composite ( **J** band at  $1.25 \mu\text{m}$ , **H** band at  $1.65 \mu\text{m}$ , **Ks** band at  $2.15 \mu\text{m}$ ). Overlaid are the  $8.7 \mu\text{m}$  contours derived from TIMMI2 observations we performed in July 2003 at ESO's 3.6-m telescope in Chile. According to our astrometry, the compact mid-infrared object near the reference position does not coincide with the (red) NIR source F1 (cf. Fig. 1), but probably traces the newly discovered object F4, i.e., the counterpart of the HMC.

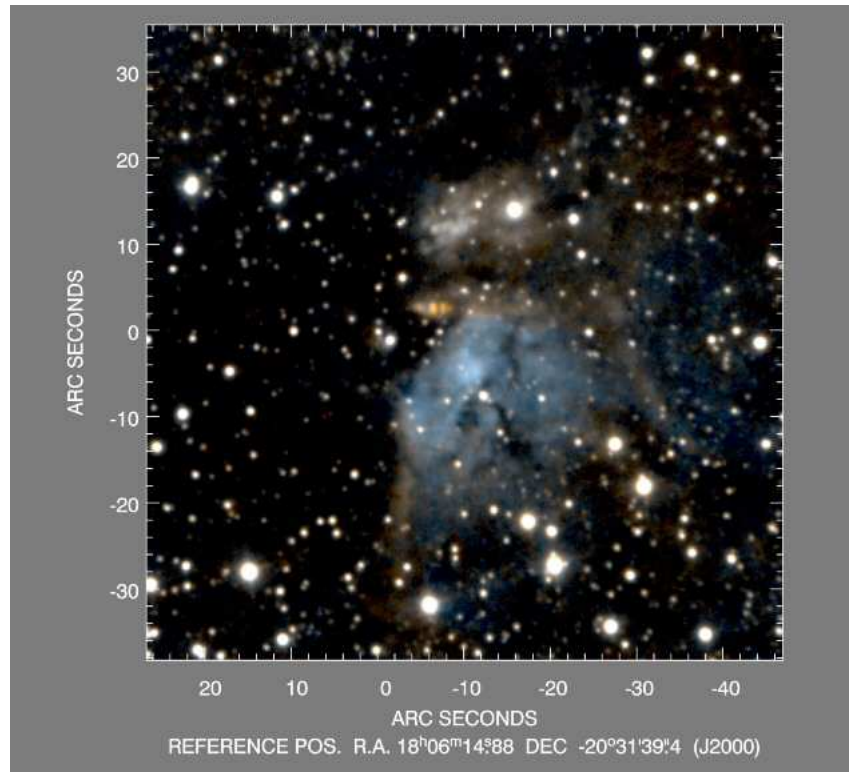


**Figure 3.** Entire view on the star-forming complex G9.62+0.19, colour-coded with the H<sub>2</sub> emission (2.12  $\mu\text{m}$ ) in red and the Br  $\gamma$  emission (2.17  $\mu\text{m}$ ) in blue. Beside the dominating (and expected) Br  $\gamma$  emission arising from the HII region (component B), this composite reveals the presence of a quite compact H<sub>2</sub> emission feature roughly in the centre of the image. The extended emission in the north (in white) is mainly reflected continuum emission.

## 2.2. GGD 27 – A splendiferous IR reflection nebula with a pumping heart

This region, which contains a deeply embedded IRAS source in its centre, is associated with the Herbig–Harro objects HH80/81 and HH80-North ( $d \sim 1.7$  kpc). An IR reflection nebula surrounds the more enshrouded inner region. The central object was finally detected in the mid-IR (Stecklum et al. 1997). Martí et al. (1993) revealed a large and well-collimated thermal radio jet emanating from the central source. This jet-driving source is a prime candidate for the search of an accretion disk around a newly formed massive star.

Our new ISAAC NIR narrow-band and thermal infrared data show the nebula and its power source in unprecedented detail: The reflection nebula exhibits a bipolar morphology (Fig. 4), the entire structure is roughly aligned along the NE–SW direction of the jet. A large fraction of the extended emission consists of scattered light. Localised spots of H<sub>2</sub> emission (presumably due to shocks) exist. With the VLA, we found a 7-mm emission peak, indicative of thermal dust emission, that is coincident with the embedded jet-driving source and offset from NIR features (Figs. 4 and 5). In the thermal infrared, the driving source finally becomes visible (Fig. 5). With our new ISAAC data we could detect it for the first time at a wavelength as short as 3.8  $\mu\text{m}$ .

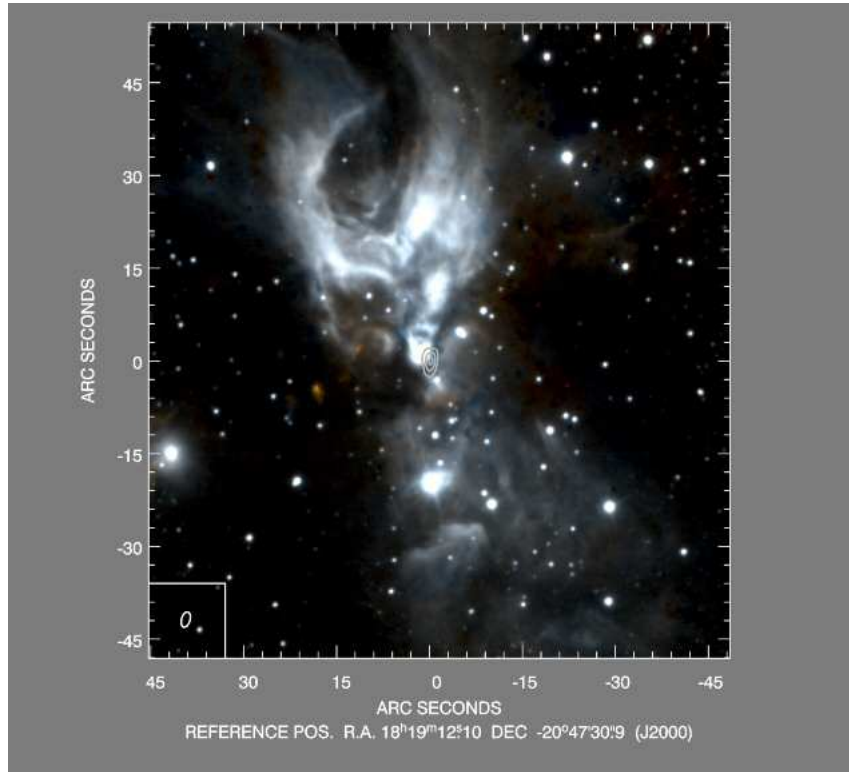


**Figure 4.** The GGD 27 reflection nebula, colour-coded with the H<sub>2</sub> emission (2.12  $\mu\text{m}$ ) in red and the Br  $\gamma$  emission (2.17  $\mu\text{m}$ ) in blue. The overlaid contours denote the sole emission peak at 7 mm, revealed by our VLA D-array data which is coincident with the jet-driving source. It is clearly offset from the neighbouring NIR feature IRS2.

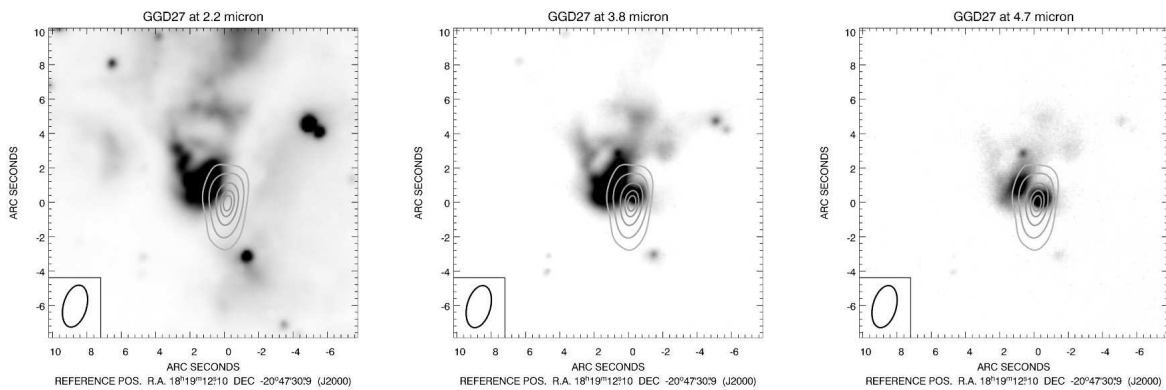


**Figure 5.** The centre of the star-forming region GGD27 around IRS2. While still hidden at 2.2 micron, the actual power source of the region finally becomes visible in the thermal infrared. Again, the contours trace the 7-mm emission which turns out to be in good positional agreement with the embedded infrared source.



### 3. Conclusions

As a result of our ISAAC observations, several southern high-mass star-forming regions could be investigated in greater detail than before. The large degree of complexity has been revealed. We could show that the actual interesting sources often remain invisible in the near-infrared due to their deep embedding in the dense gas and dust configurations of the natal molecular clouds. Therefore, imaging in the thermal infrared turned out to be extremely useful to trace these secluded objects. Hence, multi-wavelength data sets were pivotal to get the whole picture. Accurate astrometry could be applied which has a great impact on the interpretation of the data. One of the lessons learned is that the relation between infrared and radio emission is sometimes not as clear-cut as it might seem. Thus, careful and detailed investigations like the presented ISAAC campaign are crucial for the deeper understanding of the mechanisms of massive star formation. However, the ISAAC results represent only an intermediate step. Still higher resolution is required to study all the details of massive star formation – a task for powerful Adaptive Optics systems on telescopes of the 8-m class.

**Acknowledgements.** H. L. and B. S. were supported by the German *Deutsche Forschungsgemeinschaft*, *DFG*, project number STE 605/17-2. P. H. acknowledges partial support from the Research Corporation grant No CC 4996, as well as from the NSF grant AST-0098524. We are indebted to Esteban Araya for the reduction the VLA 7-mm map of GGD27. See his poster contribution about the high-mass star-forming region G31.41+0.31, also on this web page.

### References

- Cesaroni, R., Churchwell, E., Hofner, P., Walmsley, C. M., & Kurtz, S. 1994, *A&A*, 288, 903
- De Buizer, J. M., Radomski, J. T., Telesco, Ch. M., & Pina, R. K. 2003, *ApJ*, accepted (astro-ph/0307155)
- Hofner, P., Kurtz, S., Churchwell, E., Walmsley, C. M., & Cesaroni, R. 1994, *ApJ*, 429, L85
- Hofner, P., Kurtz, S., Churchwell, E., Walmsley, C. M., & Cesaroni, R. 1996, *ApJ*, 460, 359
- Hofner, P., Wiesemeyer, H., & Henning, Th. 2001, *ApJ*, 549, 425
- Linz, H., Stecklum, B., Henning, Th., Hofner, P., & Brandl, B., 2003, *A&A*, submitted
- Martí, J., Rodríguez, L. F., & Reipurth, B. 1993, *ApJ*, 416, 208
- Moorwood, A. F. 1997, *Proc. SPIE*, Vol. 2871, ed. A. L. Ardeberg, 1146
- Osorio, M., Lizano, S., & D’Alessio, P. 1999, *ApJ*, 525, 808
- Stecklum, B., Feldt, M., Richichi, A., Calamai, G., & Lagage, P. O. 1997, *ApJ*, 479, 339
- Testi, L., Felli, M., Persi, P., & Roth, M. 1998, *A&A*, 329, 233